

Scientific paper

A Novel Electrochemical CuO-Nanostructure Platform for Simultaneous Determination of 6-thioguanine and 5-fluorouracil Anticancer Drugs

Masoud Fouladgar¹¹ Department of Biochemistry, Falavarjan Branch, Islamic Azad University, Isfahan, Iran.* Corresponding author: E-mail: Fouladgar@iaufala.ac.ir;
Tel: +98 9131295016

Received: 01-23-2019

Abstract

Analysis of anticancer drugs is very important and necessary for the correct administration of them in the human body. Electrochemical behavior of 6-thioguanine (6-TG) has been studied using a carbon paste electrode modified by 1-ethyl-3-methylimidazolium tetrafluoroborate (ionic liquid) (1E3MIBF4) and CuO nanoparticles (CuO/1E3MIBF4/CPE). Using square wave voltammetry showed the linear relation between net anodic current and concentration of 6-TG in the range of 70 nmol L⁻¹ to 520 μmol L⁻¹ 6-TG with the detection limit of 20 nmol L⁻¹ 6-TG. The proposed modified electrode had excellent repeatability (RSD = 1.31%, n = 5) and long term stability (2.9% deviation in 25 days). The diffusion coefficient of 6-TG on the CuO/1E3MIBF4/CPE was found to be 1.54 × 10⁻⁵ cm²s⁻¹. The CuO/1E3MIBF4/CPE was successfully applied for the determination of 6-TG in real samples. In addition, the anodic peaks of 6-TG and fluorouracil (5-FU) in their mixture can be well separated using CuO/1E3MIBF4/CPE and simultaneous determination of them was studied.

Keywords: 6-Thioguanine; 5-Fluorouracil; CuO nanoparticles; 1-ethyl-3-methylimidazolium tetrafluoroborate; voltammetry

1. Introduction

6-Thioguanine (6-TG) is a common anticancer and antitumor drug which is an analogue of the physiological purines, guanine and hypoxanthine. In addition, thioguanine has been applied for treatment of hematological malignancies, psoriasis and inflammatory bowel disease, such as Crohn's disease. It has interaction with DNA and RNA and using it may have several side effects. Its main side effects are on the liver and it can cause hemotoxicity as well.¹ Oral administered of 6-TG is poorly absorbed and about 30% of administered dose being bioavailable. In hepatic metabolism of 6-TG, a methyl group is added to the sulfhydryl group of 6-TG.²

5-Fluorouracil (5-FU) is an antimetabolite agent same as 6-thioguanine that is being used for treatment of cancer. This group of drugs disrupts nucleic acid synthesis and is toxic to normal cells. It is a fluorinated pyrimidine and inhibits synthesis of DNA by blocking thymidylate synthetase. It is used in treatment of small tumors for which surgery is contraindicated. Particularly it is em-

ployed for the treatment of metastatic carcinomas of the breast, gastrointestinal tract, head and neck, and pancreas. Administered 5-Fluorouracil undergoes hepatic metabolism and about 10% of administered dose excretes unchanged in urine.² Both 6-TG and 5-FU are in the list of World Health Organization's List of Essential Medicines.³

Control of the adverse side effects of drugs and determination the pharmacokinetics properties are the important reasons to measurement the drugs in pharmaceutical samples and in biological samples too. In this regard many analytical methods have been reported to analysis drug samples including electrochemical methods.^{4,5} Many modified electrochemical sensors have been suggested for determination and studying interactions of 6-TG. Madueno et al. have been studied electrochemical oxidation of this anticancer drug (6-TG) including adsorption and phase formation on the mercury electrode.⁶ Wang et al. could measure 6-TG by modified gold electrode with DNA. Potassium ferricyanate was used as an electroactive indicator to probe the interaction between 6-TG and DNA.⁷ Ensafi et al. used the ability of 6-TG to form com-

plex with Cu(II) and cathodic stripping on the mercury electrode.⁸ Beitollahi et al. reported application of 2,7-bis(ferrocenyl ethyl)fluoren-9-one as a modifier of carbon paste electrode. They determined 6-TG based on electrocatalytic effect of modifier.⁹ Eksin et al. studied interaction between 6-TG and ss-DNA on the pencil graphite electrode and obtained data confirmed interactions between 6-TG and ss-DNA.¹⁰ Beitollahi et al. reported determination of 6-TG and folic acid using amplified sensors with ZnO-CuO nanoplates and 2-chlorobenzoyl ferrocene.¹¹

To improve the analytical features of the electrochemical methods, applied electrodes have been modified with different materials.^{12–14} In recent years, nanomaterials have been widely used in electrochemical analysis methods.^{15–20} Electrochemical sensors amplified with conductive materials help to improving sensitivity of electroactive materials sensors and also increase the diversity of them.^{21–26} In between, nanomaterials with different and unique properties showed more attention for modification of electrochemical sensors.^{27–31} One of the effects of application of nanomaterials is due to the change in the active surface area of electrodes.^{32–34} This effect and some other effects that appear when the size of particles decreases to nanoscale, cause to improve performance of electrochemical methods.³⁵ However, application of nanoparticles may have disadvantage effect on the electrochemical signals and increases background currents. Copper oxide nanoparticles are semiconductor metal that not only have special electrical and magnetic properties but also have great biological properties including effective antimicrobial action. Wide applications of CuO nanoparticles has caused significant advance in synthesis approaches of CuO nanoparticles.³⁶ Zeta potential values of CuO nanoparticles are negative or positive depending on pH of solution and can effect adsorption of electroactive species and improve electrochemical signals.³⁷

In addition, using electrically conducting liquids especially ionic liquids in the structure of paste electrodes, improves the sensitivity of the electrodes.^{38–46} 1-ethyl-3-methylimidazolium tetrafluoroborate is a room temperature ionic liquid that has suitable electrochemical stability for voltammetric aspects. It has wide voltage range of the electrochemical window, which allows electrochemical studies on various electroactive compounds.^{47,48}

In this work, synthesized CuO nanoparticles and 1E3MIBF₄ were used for amplification of modified sensor. Composition of CuO/1E3MIBF₄/CPE was optimized and CuO/1E3MIBF₄/CPE was suggested to determine 6-TG in real samples. In addition, simultaneous determination of 6-TG and 5-FU was investigated using modified electrode.

2. Experimental

2.1. Materials and Devices

All chemical compounds (6-thioguanine, 5-fluorouracil, phosphoric acid, 1-ethyl-3-methylimidazolium

tetrafluoroborate, copper(II) acetate, paraffin oil, sodium hydroxide and graphite powder) were purchased from Sigma-Aldrich Company in analytical grade and they were used as received without any further purification. Ultrapure water (18.2 MΩ cm, Mili-Q) was used for preparation of solutions. Phosphate buffer solutions were prepared by mixing adequate amounts of 0.1 mol L⁻¹ sodium dihydrogen phosphate and 0.1 mol L⁻¹ sodium hydrogen phosphate solutions. To prepare 6-TG standard solution (1 × 10⁻³ mol L⁻¹), adequate amount of 6-TG was dissolved in warm (35–40 °C) 1:1 (v/v) water-ethanol solution.

Electrochemical measurements were executed by Autolab PGSTAT 101 potentiostat/galvanostat (Metrohm, Netherlands) in a conventional electrochemical cell (50 ml). An Ag/AgCl electrode and a platinum wire electrode were applied as reference electrode and counter electrode, respectively. CuO/1E3MIBF₄/CPE was used as working electrode.

2.2. Real Sample Preparation

To prepare the tablets sample, five tablets were exactly weighed. Then the tablets were grinded and were completely homogenized. Then a required amount of the powder was transferred to the 100 ml beaker and about 80 ml of warm (35–40 °C) 1:1 (v/v) water-ethanol solution was added. The mixture was stirred magnetically and ultrasonicated (15 min) till the powder was dissolved. Afterward, the solution was filtered by filter paper and transferred to a flask and diluted to 100 ml with water-ethanol solution. For electrochemical measurement, adequate amount of resultant solution was transfer to electrochemical cell containing 10 ml of phosphate buffer solution (pH = 7.0).

The spiked dextrose-saline solution was prepared by mixing dextrose-saline solution with the same volume of phosphate buffer solution (pH = 7.0). Then 10 ml of resultant solution was added to the electrochemical cell and adequate amount of standard solution of 6-TG was added.

2.3. Nanoparticle Synthesis

200 ml of 0.2 mol L⁻¹ copper(II)acetate mixed with 2 ml acetic acid solution and mixture was heated until it came to boil. Then 30 ml of 0.8 mol L⁻¹ NaOH were added to the mixture. The color of the solution changed from blue to black. Afterwards, the mixture was boiled for 2 h. After cooling the mixture in the air, it was centrifuged into solid and water and the obtained solid was separated and washed.

2.4. Fabrication of CuO/1E3MIBF₄/CPE

The composition of CuO/1E3MIBF₄/CPE was optimized and optimum composition contained 10% 1E

3MIBF₄ and 6% nanoparticles. Accordingly, a mixture including 10% 1E3MIBF₄ as ionic liquid, 6% CuO nanoparticles and 84% graphite powder was prepared. About 1 ml of diethyl ether was added to the mixture and the mixture was mixed until a uniform mixture obtained. After vaporization of diethylether, a suitable amount of viscose paraffin was added to the mixture and components were mixed and the obtained paste was inserted into the glass tube in the presence of copper wire.

2. 5. Recommended Procedure

Prepared modified electrode was polished with a white and clean paper. To measure blank signal, ten milliliters of buffer solution (pH = 7.0) were transferred to the electrochemical cell. Then, the square wave voltammogram was recorded from 0.35 to 1.25 V *vs.* Ag/AgCl (Frequency 10 Hz). Afterward, different amounts of standard solutions of 6-TG and/or 5-FU were added to the cell and square wave voltammograms were recorded again to get the analytical signal. The difference between the blank and the analytical signal was obtained as a net peak current. Calibration plot was constructed by plotting net currents *vs.* concentration of drugs.

3. Results and Discussion

3. 1. Investigation of Synthesized Nanoparticles

Scanning electron microscopy (SEM) of synthesized nanoparticles confirmed synthesis of uniform spherical particles with nanoscale size (Figure 1.a). In addition, obtained Energy-dispersive X-ray (EDX) spectrum from synthesized nanoparticles confirmed the existence of only oxygen and copper in the composition of nanoparticles (Figure 1.b).

3. 2. pH effect

According to the previous electrochemical reported papers for analysis of 6-TG,⁴⁹ we guessed the pH dependent electro-oxidation mechanism for determination of 6-TG at a surface of electrode. Therefore, linear sweep voltammograms of 6-TG (100 μmol L⁻¹) were recorded in the pHs range of 5–8. As can be seen in Figure 2 (inset), increasing pH of solution causes the shift of oxidation peak potential to negative potentials. The slope of plot of potential versus pH was -61.2 mV/pH, which is close to anticipated Nernstian value (Figure 2). Consequently, this indicates that the electro-oxidation of 6-TG occurred in the presence of equal value of proton and electron. The obtained result agrees with the suggested mechanism for electro-oxidation of 6-TG (Scheme 1).⁴⁹

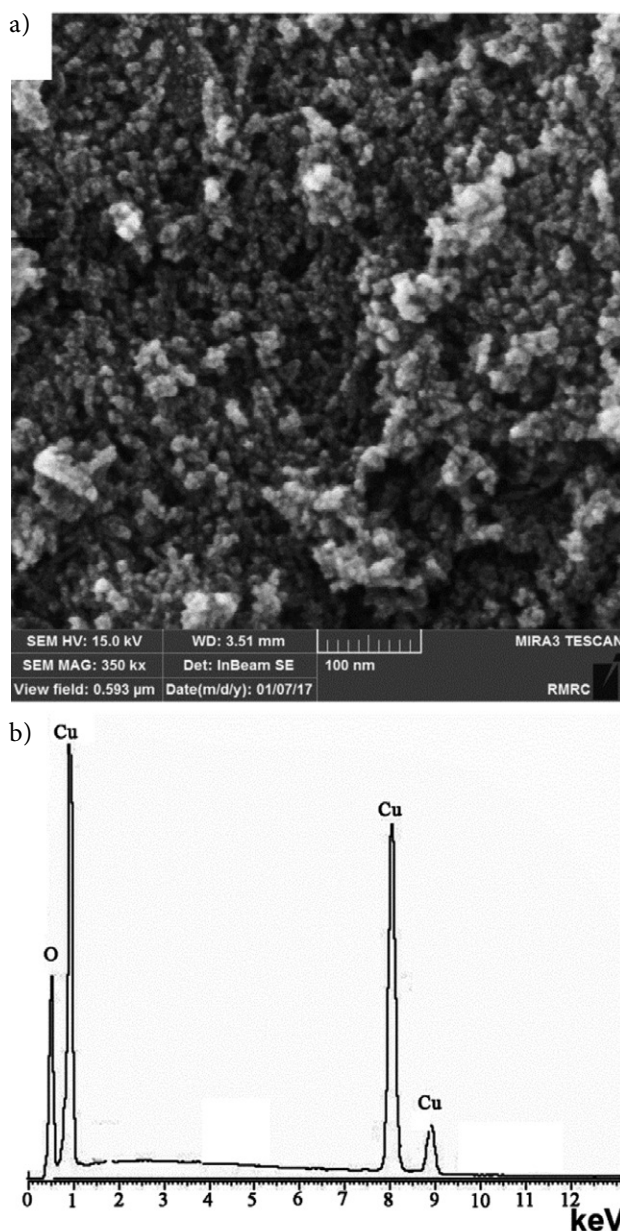


Figure 1. a) SEM image b) EDX spectrum of synthesized CuO nanoparticles

3. 3. Effect of Modification

In this step, we investigated the synergic effect of modifiers on the 6-TG electro-oxidation signal by recording the linear sweep voltammograms 6-TG (100 μmol L⁻¹) at a surface of CuO/1E3MIBF₄/CPE (curve a), 1E3MIBF₄/CPE (curve b), CuO/CPE (curve c) and CPE (curve d). As can be seen in Figure 3, addition of CuO nanoparticles caused increasing oxidation current and shifting peak potential toward lower potentials. Addition of ionic liquid into the carbon paste had similar effects. Synergy between effects of addition of nanoparticles and ionic liquid caused to achieve maximum peak current and lower overpotential (Figure 3. a). In addition, the current density in-

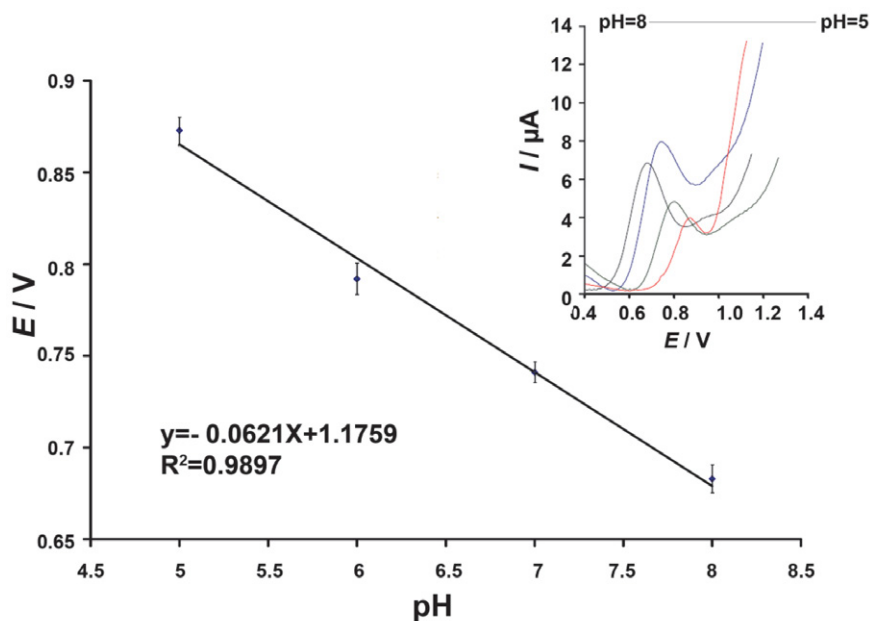
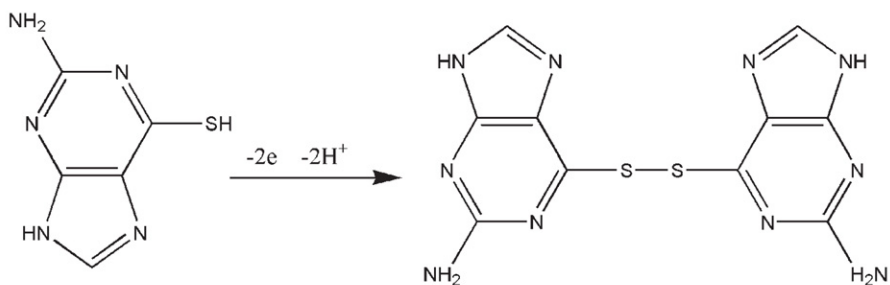


Figure 2. Plot of potential vs. pH for the electrooxidation of $100 \mu\text{mol L}^{-1}$ 6-TG at $\text{CuO}/1\text{E}3\text{MIBF}_4/\text{CPE}$. Inset: Linear sweep voltammograms of $100 \mu\text{mol L}^{-1}$ 6-TG with different pHs (scan rate = 100 mV s^{-1}).



Scheme 1. Proposed mechanism for oxidation of 6-TG on the electrode.

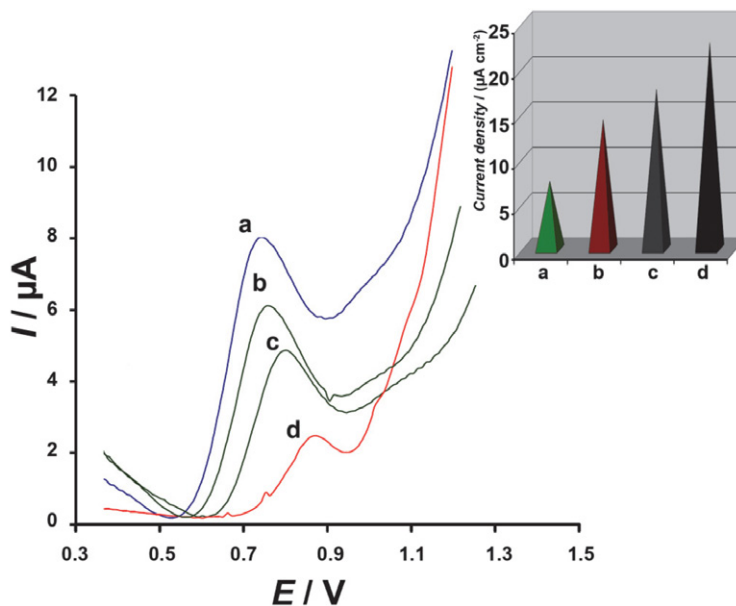


Figure 3. Linear sweep voltammograms of (a) $\text{CuO}/1\text{E}3\text{MIBF}_4/\text{CPE}$, (b) $1\text{E}3\text{MIBF}_4/\text{CPE}$, (c) CuO/CPE , and (d) CPE in the presence of $100 \mu\text{mol L}^{-1}$ 6-TG at pH 7.0. Inset: the current densities derived from voltammograms responses at same electrodes.

creased by moving CPE to CuO/1E3MIBF₄/CPE (Figure 3. inset).

These effects may be relative to the conductivity effect of CuO nanoparticles and 1E3MIBF₄ at a surface CPE. In addition, the active surface area of modified and non-modified electrodes CuO/1E3MIBF₄/CPE, 1E3MIBF₄/CPE, CuO/CPE and CPE was obtained based on the Randles–Sevcik equation (in the presence of 1 mM K₄Fe(CN)₆).³² The active surface areas of CPE, CuO/CPE, 1E3MIBF₄/CPE and CuO/1E3MIBF₄/CPE were calculated equals; 0.28, 0.31, 0.32 and 0.33 cm², respectively.

3. 4. Electrochemical Investigations

Linear sweep voltammograms of 6-TG (300 μmol L⁻¹) at CuO/1E3MIBF₄/CPE were recorded in the scan range between 10-100 mVs⁻¹ (Figure 4-a inset). Linear relation between peak currents and square root of scan

rates confirmed that the electrode process was controlled under the diffusion step. In addition, a kinetic limitation can be observed in this investigation due to shifted oxidation peak potential toward positive value. Also, the value of charge transfer coefficient (α) was obtained ~ 0.8 using slope of Tafel plot (Figure 4-b).

Chronoamperometry was also employed for investigation of 6-TG (300 and 500 μmol L⁻¹) electro-oxidation at CuO/1E3MIBF₄/CPE by applying single potential step 800 mV at CuO/1E3MIBF₄/CPE. From the slopes of plots of I (current) versus $t^{-1/2}$ (Figure 5), the average of diffusion coefficient of 6-TG was found to be 1.54×10^{-5} cm²s⁻¹ (Cottrell equation). Since electrode reaction is diffusion-controlled, anodic current is controlled by diffusion and hence depends on the diffusion coefficient. Modification of electrode causes increasing diffusion coefficient which in turn leads to increasing anodic current.

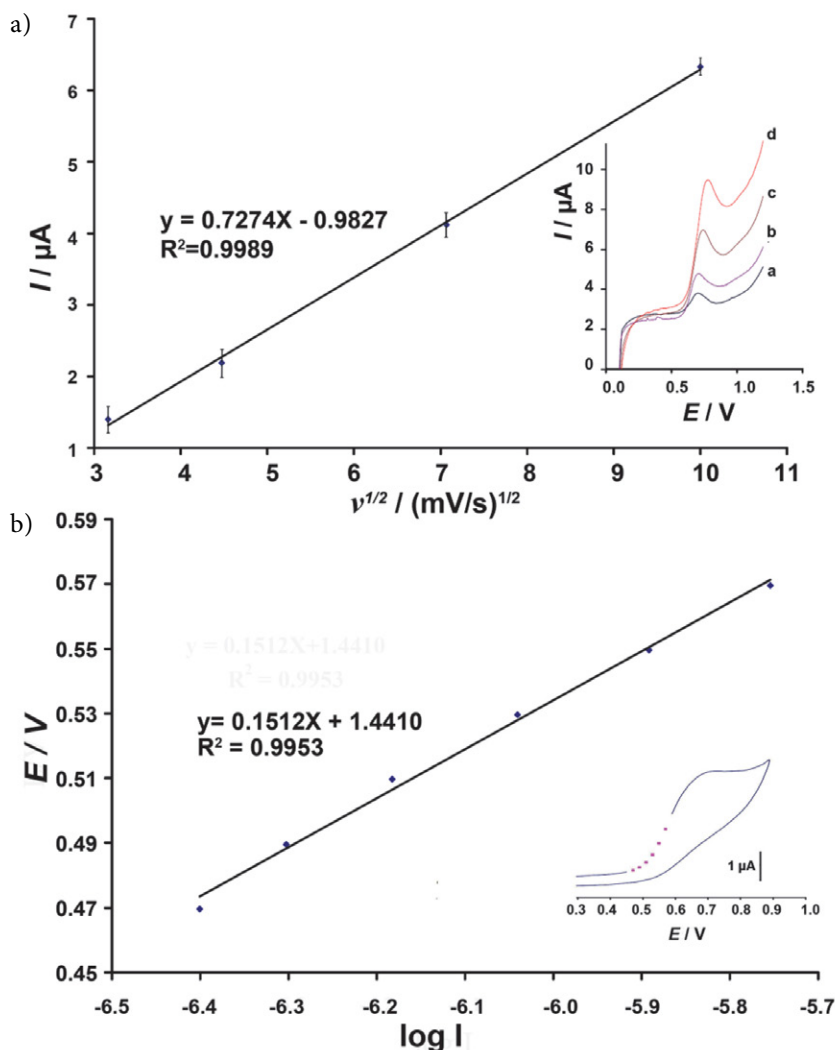


Figure 4. a) The Plot of I_{pa} vs. $v^{1/2}$ for electro-oxidation of 300 μmol L⁻¹ 6-TG (pH = 7.0). Inset; linear sweep voltammograms of CuO/1E3MIBF₄/CPE containing 300 μmol L⁻¹ 6-TG at various scan rates; a-d correspond to 10, 20, 50 and 100 mVs⁻¹, respectively. b) Tafel plot for 300 μmol L⁻¹ (pH = 7.0) 6-TG at CuO/1E3MIBF₄/CPE. Inset: Corresponding cyclic voltammogram

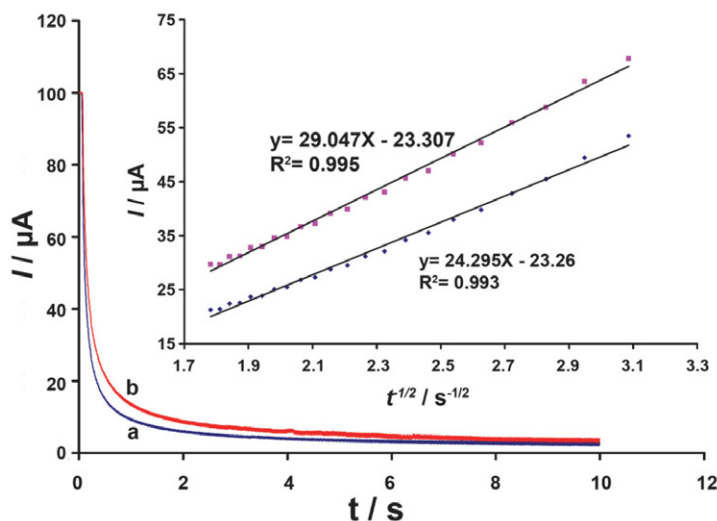


Figure 5. Chronoamperograms obtained at CuO/1E3MIBF₄/CPE in the presence of a) 300; and b) 500 μmol L⁻¹ of 6-TG in the buffer solution (pH 7.0). Inset: Cottrell's plot for the data from the chronoamperograms.

4. Analytical Features

In order to obtain calibration curve, square wave voltammograms (SWV) of solutions with different 6-TG concentrations were recorded at CuO/1E3MIBF₄/CPE. Plot of net oxidation peak current versus concentration was linear in the range of 70 nmol L⁻¹ to 520 μmol L⁻¹ 6-TG with the regression equation being $I_p(\mu\text{A}) = 0.076C_{6\text{-TG}} + 0.174$ ($R^2 = 0.998$) and detection limit of the method 20 nmol L⁻¹ 6-TG ($3S_b/m$). This value of linear dynamic range or limit of detection compared with previous electrochemical sensor and results showed better analytical ability for proposed sensor (Table 1).

The relative standard deviation for square wave signals of 25 μmol L⁻¹ 6-TG at the surface of CuO/1E3MIBF₄/CPE was 1.31% ($n = 5$), which confirmed excellent repeatability. The stability of CuO/1E3MIBF₄/CPE was checked

by recorded square wave voltammograms of 25 μmol L⁻¹ 6-TG over a period of 25 days. Compared to its first oxidation current, only 2.9% deviation was recorded when CuO/1E3MIBF₄/CPE was used daily and stored in the laboratory. This suggests that CuO/1E3MIBF₄/CPE possesses long-term stability.

Table 2. Interference study for analysis of 50 μmol L⁻¹ 6-TG

Species	Tolerance limits (mole ratio)
Glucose	850
Na ⁺ , Br ⁻ , Cl ⁻ , K ⁺ , Ascorbic acid*	550
Phenyl alanine, Glycine, Methionine	400
Starch	Saturation

* After addition of 1 mmol L⁻¹ ascorbic oxidize

Table 1. Characteristics of several electrochemical methods for determination of 6-TG

Technique	Electrochemical Method	Linear dynamic range	Detection limit	Ref.
Study self-assembled monolayer of 6-TG on mercury electrode	cyclic and ac voltammetry	–	–	6
DNA-modified gold electrode	differential pulse stripping voltammetry	2×10^{-8} – 8×10^{-7} mol L ⁻¹	6×10^{-9} mol L ⁻¹	7
Complex formation and adsorption on mercury electrode	cathodic adsorptive stripping	0.15–180 nmol L ⁻¹	0.08 n mol L ⁻¹	8
Electrocatalyst	differential pulse voltammetry	0.06–10 μmol L ⁻¹ and 10–160 μmol L ⁻¹	22 nmol L ⁻¹	50
Study interaction between 6-TG and DNA	differential pulse voltammetry, electrochemical impedance spectroscopy	–	–	10
Electrocatalyst and using ZnO-CuO nanoplates	square wave voltammetric	0.05 to 200 μmol L ⁻¹	25 n mol L ⁻¹	11
Modification of carbon paste with CuO nano particles and ionic liquid	square wave voltammetric	0.07 to 520 μmol L ⁻¹	20 n mol L ⁻¹	this work

Table 3. Determination of 6-TG in real samples (n = 5)

Sample	Added ($\mu\text{mol L}^{-1}$)	Expected ($\mu\text{mol L}^{-1}$)	Founded ($\mu\text{mol L}^{-1}$)	Recovery %	Published method ($\mu\text{mol L}^{-1}$)
Tablet*	–	5	4.92 ± 0.35	98.4	4.95 ± 0.28
	10	15	15.63 ± 0.75	104.2	15.74 ± 0.98
Intravenous solution**	–	–	< Limit of detection		
	20	20	20.75 ± 0.82	103.7	19.75 ± 1.01

±Shows the standard deviation * Kwaliti Pharmaceuticals limited, India. **Dextrose (3.33 %), saline (0.3 %), I.P.P.C.(Iranian Parenteral & Pharmaceutical Co), Tehran, Iran.

To study the influence of various substances which may potentially interfere with the determination of 6-TG, the oxidation current of $50 \mu\text{mol L}^{-1}$ 6-TG was measured in the presence of different concentrations of interfering species and was compared with current that obtained from 6-TG solution by acceptable error $\pm 5\%$. The results are shown in Table 2 and confirm selectivity of CuO/1E-3MIBF₄/CPE for the analysis of 6-TG.

To study the application of CuO/1E3MIBF₄/CPE for analysis of 6-TG in real samples, the CuO/1E3MIBF₄/CPE was applied for the determination of 6-TG in tablets and intravenous dextrose-saline solutions (Table 3).

In addition, changing the concentration of each one had no effect on the peak current of another one. Therefore, simultaneous determination was performed by simultaneously changing the concentrations of 6-TG and 5-FU and recording the SWVs. Figure 6 shows the calibration curves of 6-TG and 5-FU. The current sensitivities towards 6-TG in the presence and in the absence of 5-FU were found to be approximately equal which confirms that the oxidation processes of 6-TG and 5-FU at CuO/1E3MIBF₄/CPE are independent and simultaneous or independent measurements of two compounds are, therefore, possible without any interference.

5. Simultaneous Determination of 6-TG and 5-FU

Square wave voltammogram of a solution containing 6-TG and 5-FU showed two distinguished peak currents.

6. Conclusion

As a conclusion, we fabricated a novel electrochemical modified sensor amplified with CuO nanoparticles and 1E3MIBF₄ for the determination of 6-TG in the presence

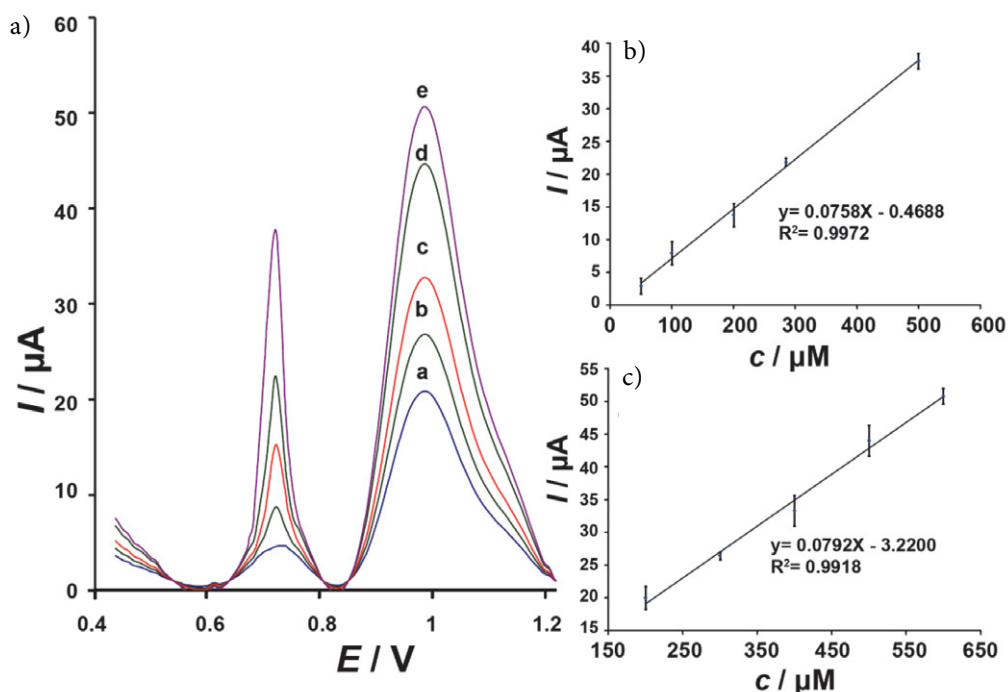


Figure 6. Inset; SWVs of CuO/1E3MIBF₄/CPE (PBS buffer, pH 7.0) containing different concentrations of 6-TG and 5-FU in $\mu\text{mol L}^{-1}$. (a–e) 50 + 200; 100 + 300; 200 + 400; 285 + 500 and 500 + 600, respectively. B) plot of the current as a function of 6-TG concentration. C) plot of the current as a function of 5-FU concentration.

of 5-FU, as two important anticancer drugs. The CuO/1E-3MIBF₄/CPE showed good analytical ability for nanomolar determination of 6-TG. The CuO/1E3MIBF₄/CPE resolved overlapping signal of 6-TG and 5-FU at an optimum condition. The CuO/1E3MIBF₄/CPE was used for the analysis of 6-TG in real samples.

Acknowledgements

The author gratefully acknowledges Islamic Azad University, Falavarjan branch research council for support of this work.

7. References

- J. K. Aronson, Book Meyler's side effects of drugs: the international encyclopedia of adverse drug reactions and interactions, Elsevier, 2015.
- S. Enna and D. Bylund, Book xPharm: The Comprehensive Pharmacology Reference, Elsevier, 2008.
- A. Attaran, *Health Aff.* **2004**, *23*, 155–166. DOI:10.1377/hlthaff.23.3.155
- J. G. Manjunatha, *J. Surface Sci. Technol.* **2018**, *34*, 74–80. DOI:10.18311/jsst/2018/15838
- J. G. Manjunatha, *Sens. Biosensing Res.* **2017**, *16*, 79–84. DOI:10.1016/j.sbsr.2017.11.006
- R. Madueno and T. Pineda, *J. Electroanal. Chem.* **2004**, *565*, 301–310. DOI:10.1016/j.jelechem.2003.10.024
- S. F. Wang, F. Xie, R. F. Hu and H. C. Cai, *Anal. Lett.* **2006**, *39*, 1041–1052. DOI:10.1080/00032710600620328
- A. A. Ensafi and R. Hajian, *J. Brazil. Chem. Soc.* **2008**, *19*, 405–412. DOI:10.1590/S0103-50532008000300006
- H. Beitollahi, J.-B. Raoof and R. Hosseinzadeh, *Anal. Sci.* **2011**, *27*, 991–991. DOI:10.2116/analsci.27.991
- E. Eksin, G. Congur, F. Mese and A. Erdem, *J. Electroanal. Chem.* **2014**, *733*, 33–38. DOI:10.1016/j.jelechem.2014.08.012
- H. Beitollahi, S. G. Ivani and M. Torkzadeh-Mahani, *Mater. Sci. Eng., C* **2016**, *69*, 128–133. DOI:10.1016/j.msec.2016.06.064
- N. S. Prinith and J. G. Manjunatha, *Mater. Sci. Technol. Energy* **2019**, *2*, 408–416. DOI:10.1016/j.mset.2019.05.004
- J. G. Manjunatha, B. E. K. Swamy, G. P. Mamatha, C. Raril, L. N. Swamy and S. Fattepur, *Materials Today: Proceedings* **2018**, *5*, 22368–22375. DOI:10.1016/j.matpr.2018.06.604
- C. Raril and J. G. Manjunatha, *Anal. Bioanal. Electrochem.* **2018**, *10*, 372–382.
- G. Tigari, J. G. Manjunatha, C. Raril and N. Hareesha, *Chemistry Select* **2019**, *4*, 2168–2173. DOI:10.1002/slct.201803191
- N. S. Prinith, J. G. Manjunatha and C. Raril, *Anal. Bioanal. Electrochem.* **2019**, *11*, 742–756.
- J. G. Manjunatha, *Open Chem Eng J.* **2019**, *13*, 81–87. DOI:10.2174/1874123101913010081
- S. Cheraghi, M. A. Taher and H. Karimi-Maleh, *J. Food Compos. Anal.* **2017**, *62*, 254–259. DOI:10.1016/j.jfca.2017.06.006
- B. J. Sanghavi, G. Hirsch, S. P. Karna and A. K. Srivastava, *Anal. Chim. Acta* **2012**, *733*, 37–45. DOI:10.1016/j.aca.2012.05.029
- J. G. Manjuntha and G. K. Jayaprakash, *Eurasian J. Anal. Chem.* **2019**, *14*, 1–11.
- H. Karimi-Maleh and O. A. Arotiba, *J. Colloid Interface Sci.* **2020**, *560*, 208–212. DOI:10.1016/j.jcis.2019.10.007
- H. Karimi-Maleh, F. Karimi, M. Alizadeh and A. L. Sanati, *Chem. Rec.* **2020**. DOI:10.1002/tcr.201900092
- H. Karimi-Maleh, C. T. Fakude, N. Mabuba, G. M. Peleyeju and O. A. Arotiba, *J. Colloid Interface Sci.* **2019**, *554*, 603–610. DOI:10.1016/j.jcis.2019.07.047
- F. Tahernejad-Javazmi, M. Shabani-Nooshabadi and H. Karimi-Maleh, *Composites Part B: Engineering* **2019**, *172*, 666–670. DOI:10.1016/j.compositesb.2019.05.065
- A. Khodadadi, E. Faghhi-Mirzaei, H. Karimi-Maleh, A. Abbaspourrad, S. Agarwal and V. K. Gupta, *Sens. Actuators, B* **2019**, *284*, 568–574. DOI:10.1016/j.snb.2018.12.164
- Z. Shamsadin-Azad, M. A. Taher, S. Cheraghi and H. Karimi-Maleh, *J. Food Meas. Charact.* **2019**, *13*, 1781–1787. DOI:10.1007/s11694-019-00096-6
- H. Karimi-Maleh, M. Shafieizadeh, M. A. Taher, F. Opoku, E. M. Kiarri, P. P. Govender, S. Ranjbari, M. Rezapour and Y. Orooji, *J. Mol. Liq.* **2020**. DOI:10.1016/j.molliq.2019.112040
- H. Karimi-Maleh, M. Sheikhshoaei, I. Sheikhshoaei, M. Ranjbar, J. Alizadeh, N. W. Maxakato and A. Abbaspourrad, *New J. Chem.* **2019**, *43*, 2362–2367. DOI:10.1039/C8NJ05581E
- M. Miraki, H. Karimi-Maleh, M. A. Taher, S. Cheraghi, F. Karimi, S. Agarwal and V. K. Gupta, *J. Mol. Liq.* **2019**, *278*, 672–676. DOI:10.1016/j.molliq.2019.01.081
- S. Malekmohammadi, H. Hadadzadeh, S. Rezakhani and Z. Amirghofran, *ACS Biomater. Sci. Eng.* **2019**, *5*, 4405–4415. DOI:10.1021/acsbmaterials.9b00237
- Y. Akbarian, M. Shabani-Nooshabadi and H. Karimi-Maleh, *Sens. Actuators, B* **2018**, *273*, 228–233. DOI:10.1016/j.snb.2018.06.049
- M. Fouladgar and S. Mohammadzadeh, *Anal. Lett.* **2014**, *47*, 763–777. DOI:10.1080/00032719.2013.855782
- M. L. Yola and N. Atar, *Electrochim. Acta* **2014**, *119*, 24–31. DOI:10.1016/j.electacta.2013.12.028
- L. Shang, F. Zhao and B. Zeng, *Food Chem.* **2014**, *151*, 53–57. DOI:10.1016/j.foodchem.2013.11.044
- C. Jianrong, M. Yuqing, H. Nongyue, W. Xiaohua and L. Sijiao, *Biotechnol. Adv.* **2004**, *22*, 505–518. DOI:10.1016/j.biotechadv.2004.03.004
- M. E. Grigore, E. R. Biscu, A. M. Holban, M. C. Gestal and A. M. Grumezescu, *Pharmaceuticals* **2016**, *76*, 75–89. DOI:10.3390/ph9040075
- A. El-Trass, H. ElShamy, I. El-Mehasseb and M. El-Kemary, *Appl. Surf. Sci.* **2012**, *258*, 2997–3001. DOI:10.1016/j.apsusc.2011.11.025
- W. Sun, M. Yang and K. Jiao, *Anal. Bioanal. Chem.* **2007**, *389*, 1283–1291. DOI:10.1007/s00216-007-1518-2
- H. Khani, M. K. Rofouei, P. Arab, V. K. Gupta and Z. Vafaei, *J. Hazard. Mater.* **2010**, *183*, 402–409. DOI:10.1016/j.jhazmat.2010.07.039

40. M. Fouladgar, *Measurement* **2016**, *86*, 141–147.
DOI:10.1016/j.measurement.2016.02.057
41. Y. Zhang and J. B. Zheng, *Electrochim. Acta* **2007**, *52*, 7210–7216. DOI:10.1016/j.electacta.2007.05.039
42. W. Sun, Y. Li, M. Yang, S. Liu and K. Jiao, *Electrochem. Commun.* **2008**, *10*, 298–301.
DOI:10.1016/j.elecom.2007.12.012
43. S. Negahban, M. Fouladgar and G. Amiri, *J. Taiwan Inst. Chem. Eng.* **2017**, *78*, 51–55. DOI:10.1016/j.jtice.2017.05.032
44. M. Ashjari, H. Karimi-Maleh, F. Ahmadpour, M. Shabani-Nooshabadi, A. Sadriani and M. A. Khalilzadeh, *J. Taiwan Inst. Chem. Eng.* **2017**, *80*, 989–996.
DOI:10.1016/j.jtice.2017.08.046
45. M. Fouladgar, *J. Electrochem. Soc.* **2016**, *163*, B38–B42.
DOI:10.1149/2.0611603jes
46. M. Fouladgar, *Sens. Actuators, B* **2016**, *230*, 456–462.
DOI:10.1016/j.snb.2016.02.094
47. M. Shamsipur, A. A. M. Beigi, M. Teymouri, S. M. Pourmourtazavi and M. Irandoust, *J. Mol. Liq.* **2010**, *157*, 43–50.
DOI:10.1016/j.molliq.2010.08.005
48. J. Fuller, R. T. Carlin and R. A. Osteryoung, *J. Electrochem. Soc.* **1997**, *144*, 3881–3886. DOI:10.1149/1.1838106
49. P. Kraske, *J. Electroanal. Chem. Interfacial Electrochem.* **1986**, *207*, 101–116. DOI:10.1016/0022-0728(86)87065-6
50. H. Karimi-Maleh, M. R. Ganjali, P. Norouzi and A. Bananezhad, *Mater. Sci. Eng., C* **2017**, *3*, 472–477.
DOI:10.1016/j.msec.2016.12.094

Povzetek

Analiza protirakovih zdravil je zelo pomembna in potrebna za njihovo pravilno uporabo v človeškem telesu. Preučevali smo elektrokemijsko obnašanje 6-tioguanina (6-TG) z uporabo elektrode iz ogljikove paste, modificirane z 1-etil-3-metilimidazolijevim tetrafluoroboratom (ionska tekočina) (1E3MIBF4) in nanodelci CuO (CuO/1E3MIBF4/CPE). Uporaba square wave voltometrije je pokazala linearno zvezo med celotnim anodnim tokom in koncentracijo 6-TG v območju od 70 nmol L⁻¹ do 520 μmol L⁻¹ 6-TG z mejo zaznave 20 nmol L⁻¹ 6-TG. Predlagana modificirana elektroda je imela odlično ponovljivost (RSD = 1,31 %, n = 5) in dolgoročno stabilnost (2,9 % odstopanje v 25 dneh). Ugotovljeno je bilo, da je koeficient difuzije 6-TG na CuO / 1E3MIBF4/CPE $1,54 \times 10^{-5}$ cm²s⁻¹. CuO/1E3MIBF4/CPE je bil uspešno uporabljen za določanje 6-TG v realnih vzorcih. Poleg tega je mogoče anodne vrhove 6-TG in fluorouracila (5-FU) v njuni mešanici dobro ločiti z uporabo CuO/1E3MIBF4/CPE in ju preučevati istočasno.



Except when otherwise noted, articles in this journal are published under the terms and conditions of the Creative Commons Attribution 4.0 International License